ARTICLES

Basal-plane incommensurate phases in hexagonal-close-packed structures

I. Luk'yanchuk*
Departamento de Fisica, Universidade Federal de Minas Gerais, Caixa Postal 702, 30161-970, Belo Horizonte, Minas Gerais, Brazil and L. D. Landau Institute for Theoretical Physics, 117940, Moscow, Russia

A. Jorio and M. A. Pimenta†
Departamento de Fisica, Universidade Federal de Minas Gerais, Caixa Postal 702, 30161-970, Belo Horizonte, Minas Gerais, Brazil
(Received 5 August 1997)

An Ising model with competing interactions is used to study the appearance of incommensurate phases in the basal plane of a hexagonal-close-packed structure. The calculated mean-field phase diagram reveals various $1q$-incommensurate and lock-in phases. The results are applied to explain the basal-plane incommensurate phase in some compounds of the $A'A''BX_4$ family, like K_2MoO_4, K_2WO_4, Rb_2WO_4, and to describe the sequence of high-temperature phase transitions in other compounds of this family. [S0163-1829(98)03909-5]

I. INTRODUCTION

The microscopic origin of incommensurate phases in ferroelectrics, magnetic materials, binary alloys, and other related systems has been a subject of interest since the early 1960's (for a review see Ref. 1). It is now well established that incommensurate modulation in the majority of those systems is caused by the frustrating competition between different interatomic or interspin forces responsible for structural or magnetic ordering.

The first approach proposed for studying frustration-induced incommensurate phases was based on the axial next-nearest-neighbor Ising (ANNNI) model with competing uniaxial nearest-neighbor (NN) and next-nearest-neighbor (NNN) interactions in which the structural units have been described by binary Ising pseudospin variables.[1–3] Depending on the coupling parameters and temperature, this model was shown to exhibit a rich diagram of commensurate and incommensurate modulated phases when the wave vector jumps between rational and irrational values of the reciprocal-lattice period, a phenomenon known as a devil's staircase.

A large variety of incommensurate systems is adequately described by the ANNNI model and its analogous models.[2–4] The common feature of these models is that the modulation occurs in the uniaxial high-symmetry direction. There are, however, examples of incommensurate phases where the wave vector is perpendicular to the high-symmetry axis and can occur in more than one equivalent direction. The appearance of this kind of incommensurate modulation was studied for the simple cubic lattice with competing NN and NNN interactions along the cubic axes and their diagonals,[5] for the simple hexagonal lattice with NN and NNN interactions,[6–8] and for distorted triangular lattice with only NN interaction.[9]

In this paper we employ the mean-field approximation to study the Ising model on the hexagonal-close-packed (hcp) lattice, where frustration is uniquely related to the topology of the lattice and is provided by the in-plane NN antiferromagnetic interaction. We show that this frustration, being stabilized by the out-plane NN interaction, gives rise to incommensurate phases with the modulation vector lying in the basal plane. We also study the phase diagram of the system when small out-plane NNN interaction is included and show that it leads to a rich sequence of phase transitions. The used mean-field consideration is complementary to the previous cluster-approximation studies of the hcp-Ising model[10,11] and of the related hexagonal honeycomb-lattice Ising model.[10,12]

Our interest in the hcp-Ising model is provided by the transition sequence in several ionic $A'A''BX_4$ compounds where the orientational ordering of BX_4 tetrahedra drives a series of structural phases including incommensurate states.[4] The variety of transitions can be explained on the basis of the hcp-Ising model where the orientational states of BX_4 tetrahedra are described by two discrete Ising variables as proposed by Kurzyński and Halawa.[13,14] The review of the recent studies of the two-spin Kurzyński and Halawa model is given in Ref. 15. We demonstrate that the rigorous treatment of the model explains the experimentally observed basal-plane incommensurate phases in some $A'A''BX_4$ compounds and several other features not explored in the previous studies.

The paper is organized as follows. In Sec. II the structural properties of the $A'A''BX_4$ family and the motivation of the hcp-Ising model are considered. In Sec. III we treat the frustrated hcp-Ising model within the mean-field approximation in order to demonstrate the appearance of basal-plane incommensurate phases. We derive the phase diagram of the system and discuss their relation with the low-temperature cluster-approximation diagram of Refs. 10–12. In Sec. IV we discuss the application of the obtained results to the experimental properties of $A'A''BX_4$ compounds at high temperatures.

Exploring the Ising model, we use the formal terminology of magnetic systems. The properties of $A'A''BX_4$ compounds are characterized by the electrostatic interaction of BX_4 tetrahedra. Consequently, the para-, ferro-, and antiferromagnetic terms of the Ising model correspond to the para-, ferro-, and antiferroelectric terms for $A'A''BX_4$ compounds.

II. COMMENSURATE AND INCOMMENSURATE PHASES IN $A'A''BX_4$ COMPOUNDS

The structures and transition sequences in the $A'A''BX_4$ family were described in detail in the review articles.[4,14] Shortly, the $A'A''BX_4$ compounds can be presented as a set of BX_4^{2-} tetrahedral anions and A''^{+} cations that are regularly placed in the sites of a hcp structure. The A'^{+} cations form a simple hexagonal lattice.

The order-disorder transitions in these compounds are related to the ordering of degenerate orientations of BX_4 tetrahedra in the $A'A''$ matrix. A possible degree of freedom is given by the vertical up/down orientation of the tetrahedron apexes and an another one by the planar orientation of the tetrahedra. Orientational ordering of the tetrahedra breaks the initial hexagonal symmetry $P6_3/mmc$ and leads to a sequence of structural transitions when temperature decreases. In the Kurzyński and Halawa model[13] the vertical and planar orientations are described by two coupled binary spin variables, the orientational ordering being provided by the interaction between neighboring tetrahedra. The ground states of the related two-spins Ising Hamiltonian were shown[13] to correspond to the experimentally observed variety of phases in the $A'A''BX_4$ compounds. There is a common hierarchy in the transition sequence of $A'A''BX_4$ compounds. The vertical orientational ordering occur at higher temperatures (typically of 600–900 K) than the planar one (below 600 K).

A characteristic feature of $A'A''BX_4$ family is the existence of the incommensurate modulations associated with tetrahedral orientation that often appear as intermediate phases at structural transformations. They can be related either to the planar or to the vertical orientational degrees of freedom of the tetrahedra and occur in the low- and in the high-temperature regions, respectively.

The incommensurate phases of the first type have been observed in a great number of $A'A''BX_4$ compounds.[4,14] They have the modulation vector directed along the pseudohexagonal axis. The appearance of this kind of incommensurate phase was proposed to be related either to a specific antisymmetric interaction of the planar orientations of tetrahedra in the unit cell[14,16–18] or to ANNNI like interaction of the tetrahedra in neighboring basal planes.[19]

The incommensurate phases of the second type are the subject of the present study. The modulation wave vector associated with the vertical tetrahedra orientation has the incommensurate component directed in the basal plane of the hcp structure. This phase occurs in alkali molybdates and tungstates K_2MoO_4, K_2WO_4, Rb_2WO_4 in the temperature interval of 590–750 K.[20–22] There is no consistent explanation of this kind of incommensurate phase although several ideas were proposed in Ref. 14. In this work we explain the appearance of the basal-plane incommensurate structure as a result of competitive interactions between the vertical orientations of neighboring tetrahedra localized in the same basal plane and in the NN basal planes, as shown in Fig. 1.

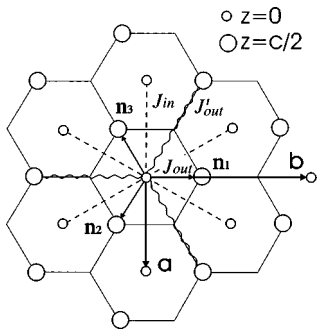

FIG. 1. J_{in}, J_{out}-NN and J'_{out} -NNN Ising interactions in hcp structure. We use the orthogonal unit cell $\mathbf{a},\mathbf{b},\mathbf{c}$ with $b=a\sqrt{3}$.

In the high-temperature region the planar orientation of the BX_4 tetrahedra is disordered and the corresponding planar spin variable is equal to zero. Thus, in this region, the Kurzyński and Halawa model is effectively reduced to the one-spin Ising model where the vertical up/down tetrahedra orientations are described by the spin variable $S_i=\pm 1$. The following analysis will be restricted to this region.

The interaction between tetrahedra has an electrostatic nature. The uniaxial anisotropy of the hcp lattice induces dipolar moments of BX_4 tetrahedra parallel to the c axis. Therefore, the interaction between the NN tetrahedra is dominanted either by their induced dipolar moments or by intrinsic octupolar moments. In both cases the interaction J_{in} between two NN BX_4 tetrahedra localized in the same basal plane favors opposite vertical orientations and therefore has an antiferromagnetic nature. In contrast, the sign of the NN out-plane interaction J_{out} depends on structural details of the system like, e.g. the ratio c/a, effective charges, etc. Thus we consider both the cases of the ferro- and antiferromagnetic interaction for J_{out}.

The mean-field minimization of the free energy given in the next section shows that the incommensurate structure does exist in a certain region of interaction parameters J_{in} and J_{out}. It appears, however, that the account of only NN interaction leads to a degeneracy between different phases. To remove this degeneracy, we introduce the weak out-plane interaction J'_{out} between NNN tetrahedra. We show that this interaction results in structures that are found experimentally.

III. MODEL AND RESULTS

We use the Ising spin variable $S_i=\pm 1$ to explore the idea about frustration-induced basal-plane incommensurate phases. The Hamiltonian is written as

$$H=\frac{1}{2}\sum_{ij} J_{ij}S_iS_j, \tag{1}$$

where

$$\begin{aligned} J_{\text{in}} &\quad \text{for the NN } \textit{in-plane} \text{ sites,} \\ J_{ij}=J_{\text{out}} &\quad \text{for the NN } \textit{out-plane} \text{ sites,} \\ J'_{\text{out}} &\quad \text{for the NNN } \textit{out-plane} \text{ sites,} \end{aligned} \tag{2}$$

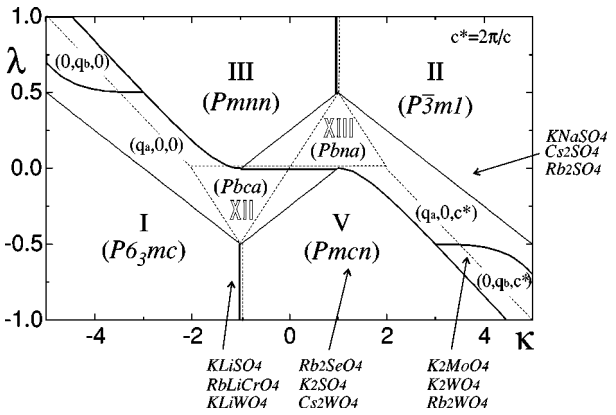

FIG. 2. Phase diagram of the hcp-Ising model as function of the NN and NNN interaction parameters $\kappa = J_{\text{out}}/J_{\text{in}}$ and $\lambda = J'_{\text{out}}/J_{\text{in}}$. Solid lines correspond to the phase diagram just below the transition from the paramagnetic state. Commensurate phases (roman numbers and corresponding symmetry groups) are also enumerated in Fig. 3 and in Table I. Incommensurate phases are given by their wave vectors (q_a, q_b, q_c). Dotted lines present the phase diagram at $T=0$. Note that phases XII and XIII existing at $T=0$ can appear from the paramagnetic states only via an intermediate incommensurate phase. We also show the possible localization of some $A'A''BX_4$ compounds.

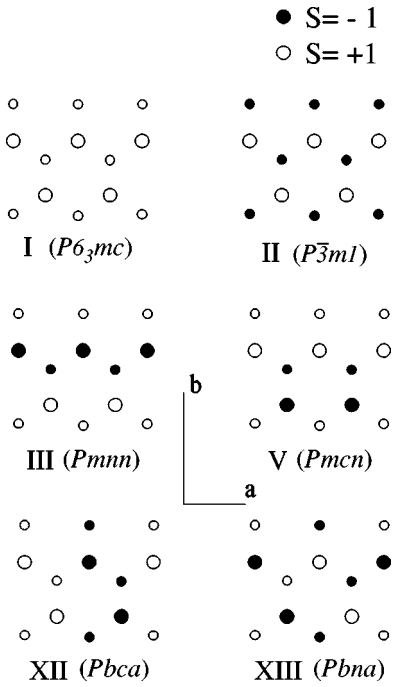

FIG. 3. Spin patterns of the commensurate phases that appear in the hcp-Ising model. Large and small circulus correspond to the spin sites in alternating planes of hcp structure. The corresponding lock-in vectors are given in Table I.

as shown in Fig. 1. The negative and positive sign of interaction constants correspond to ferro- and to antiferromagnetic interactions. As discussed in the previous section, we assume that $J_{\text{in}}>0$, and that J_{out} and J'_{out} can take both positive and negative values. It is convenient to introduce the driving dimensionless parameters: $\kappa = J_{\text{out}}/J_{\text{in}}$; $\lambda = J'_{\text{out}}/J_{\text{in}}$, the last one being assumed to be smaller than one.

Note the following properties of the Hamiltonian (1) that will be used later: (i) When the ground state for some interaction parameters κ, λ is known, the ground state for $-\kappa$, $-\lambda$ is easily obtained by inversion of signs of the spins in alternated planes. (ii) The three-dimensional hcp-Ising model can be mapped onto a two-dimensional honeycomb hexagonal lattice Ising model with NN, NNN, and NNNN interactions.[23]

The ground state of the system is found by the minimization of the free energy:

$$F = -kT \ln \mathrm{Tr} \exp(-H/kT). \tag{3}$$

At $T=0$ the problem reduces to minimization of the Ising energy $(1/2)\Sigma J_{ij} S_i S_j$ over all the possible spin configurations. The effective procedure for solving this problem was developed in Ref. 10. Using the mapping honeycomb → hcp lattice and adopting the results of Ref. 10 to our variables, we find that six phases: I, II, III, V, XII, and XIII (in the notations of Ref. 10) whose structures are shown in Fig. 3, occur at $T=0$. Their energies per one spin are

$$E_{\text{I}} = J_{\text{in}}(3+3\kappa+3\lambda), \quad E_{\text{II}} = J_{\text{in}}(3-3\kappa-3\lambda),$$

$$E_{\text{III}} = J_{\text{in}}(-1+\kappa-3\lambda), \quad E_{\text{V}} = J_{\text{in}}(-1-\kappa+3\lambda),$$

$$E_{\text{XII}} = J_{\text{in}}(-1+\kappa-\lambda), \quad E_{\text{XIII}} = J_{\text{in}}(-1-\kappa+\lambda). \tag{4}$$

The coexistence lines of these phases (shown in Fig. 2 by the dots) are defined by the equilibrium of their energies. An important observation given in Ref. 12 is that the infinite number of other degenerate ground states exists along these lines. These states become stable at finite temperature due to the entropy factor. The finite-temperature cluster-approximation study shows that the phase sequence can be quite complex (see Ref. 11 and references therein).

The low-temperature approach is useful when the values of the spins are assumed to take a fixed value of either $+1$ or -1. Close to T_c, the fluctuations of spins are important and the absolute value of the average $\sigma_i = \langle S_i \rangle$ can be substantially smaller than 1. To consider this regime, we minimize the free energy (3) within the mean-field approximation, the variables σ_i being considered as variational parameters of the model. The standard mean-field treatment[24] gives the following expression for the free energy:

$$F = \frac{1}{2}\sum_{ij} J_{ij}\sigma_i\sigma_j + kT\sum_i \int_0^{\sigma_i} \tanh^{-1} s\, ds. \tag{5}$$

In the vicinity of the transition, the absolute values of σ_i are much smaller than 1. Expanding Eq. (5) in a Taylor series we obtain the Ising-like expression with additional nonlinear terms σ_i^4:

$$F = \frac{kT}{2}\sum_i \sigma_i^2 + \frac{1}{2}\sum_{ij} J_{ij}\sigma_i\sigma_j + \frac{kT}{12}\sum_i \sigma_i^4. \tag{6}$$

Note that, unlike the discrete Ising spins $S_i = \pm 1$, the variables σ_i sweep the continuous spectrum between $+1$ and -1. Expression (6) with arbitrary coefficients is frequently used as a starting phenomenological functional for considering of incommensurate phases in systems with competing interactions.[1,6–8,14] We use this expression as a basic func-

tional that provides the phase diagram of the system. The critical temperature of the transition is given by the highest value of T where the functional (6) first becomes unstable with respect to formation of the pattern of nonzero σ_i.

Let us calculate the critical temperature and the phase diagram below the transition as a function of the interaction parameters κ,λ. It is convenient to work with the Fourier transformed variables $\sigma_q=\Sigma_i\sigma_i\exp(iqr_i)$. Fourier decomposition of Eq. (6) gives the following energy per one spin:

$$f=\frac{1}{2}\sum_q (kT+2J(q))\sigma_q\sigma_{-q}+\frac{kT}{4}\sum_q (\sigma_q\sigma_{-q})^2 + \frac{kT}{4}\sum_{q\neq q'} \sigma_q\sigma_{-q}\sigma_{q'}\sigma_{-q'}, \tag{7}$$

where

$$J(q)=J_{\rm in}[\varepsilon'(n_i-n_j)+\kappa\varepsilon(n_i)\cos q_z+\lambda\varepsilon_c(2n_i)\cos q_z], \tag{8}$$

and

$$\varepsilon(n_i)=\cos qn_1+\cos qn_2+\cos qn_3,$$

$$\varepsilon'(n_i-n_j)=\cos q(n_1-n_2)+\cos q(n_2-n_3)+\cos q(n_3-n_1).$$

We take $n_1=(0,b/3,0)$, $n_2=(a/2,-b/6,0)$, $n_3=(-a/2,-b/6,0)$ as shown in Fig. 1.

An important assumption was made that expression (7) contains no umklapp terms provided by commensurate modulation of the lock-in phases. Actually, the only phases that give this contribution are these with modulation vector $q=(0,0,0)$, $(0,0,2\pi/c)$, $(0,2\pi/b,0)$, $(0,2\pi/b,2\pi/c)$. Their spin configuration σ_j corresponds to the states I, II, III, and V of Fig. 3 with equal in-site amplitudes $\sigma=|\sigma_j|$. Free energy of these states will be calculated in a more direct way later.

The finite-q incommensurate structure becomes stable when the coefficient $kT+2J(q)$ is negative. Softening of $kT+2J(q)$ occurs simultaneously in several symmetry equivalent points of the q space. The resulting state is provided by the superposition of the corresponding degenerate plane waves that can give either a $1q$ stripe phase, or a multi-q, double-periodic phase. Later we will show that the $1q$ phase is more preferable. The modulation amplitude σ_q is a complex value satisfying $\sigma_q=\sigma^*_{-q}$. Since the functional (7) does not lock its phase we consider σ_q to be real.

The transition temperature and the modulation vector are defined by $kT_{\rm inc}=-\min_{\{q\}}2J(q)$. We found that the q_c component of the modulation vector q is always commensurate with the reciprocal-lattice vector $c^*=2\pi/c$ and takes the values of either 0 or $2\pi/c$. The incommensurate modulation appears in the basal plane along either the a or b symmetry directions. Four incommensurate phases $(q_a,0,0)$, $(q_a,0,2\pi/c)$, $(0,q_b,0)$, and $(0,q_b,2\pi/c)$ are possible.

The critical temperatures for the phases $(q_a,0,0)$ and $(q_a,0,2\pi/c)$ are given by

$$kT_a^{\pm}/J_{\rm in}=\frac{(\kappa-2\lambda)^2}{1\pm2\lambda}+3, \tag{9}$$

where the upper sign corresponds to $q_c=0$ and the lower one to $q_c=2\pi/c$. The modulation vector

$$q_a=\frac{2}{a}\arccos\left(\frac{1\pm\kappa}{2\pm4\lambda}\right) \tag{10}$$

changes from $q_a=0$ (lock-in phases I or II) to $q_a=2\pi/a$ (lock-in phases V or III).

The critical temperatures for the phases $(0,q_b,0)$ and $(0,q_b,2\pi/c)$ are given by

$$kT_b^{\pm}/J_{in}=-4[\pm4\lambda x^4+4x^3\pm(\kappa-2\lambda)x^2+4(\pm\kappa-3)x \mp(\kappa+\lambda)+1], \tag{11}$$

where

$$x=\pm\{(-3\pm2\lambda)+[(-3\pm2\lambda)^2-8\lambda(\kappa\mp3)]^{1/2}\}/8\lambda.$$

The modulation vector

$$q_b=\frac{2}{b}\arccos x \tag{12}$$

changes from $q_b=0$ (lock-in phases I or II) to $q_b=2\pi/b$ (lock-in phases V or III).

The incommensurate phases can exist only in that region of parameters κ and λ when the arguments of arccos in Eqs. (10) and in (12) are between $+1$ and -1.

Depending on the interaction parameters κ and λ, all four incommensurate phases can be stable. To find the regions of their stability one should compare $T_{\rm inc}=T_{a,b}^{\pm}$ with the critical temperatures of the lock-in phases I, II, III, V, XII, and XIII. The later is found directly from Eq. (6) since the necessary summation $\Sigma J_{ij}\sigma_i\sigma_j$ was already performed when calculating Eq. (4). For the free energy of the lock-in phases we obtain

$$f_{\rm com}=\frac{1}{2}(kT+2E_{\rm com})\sigma^2+\frac{kT}{12}\sigma^4, \tag{13}$$

where $E_{\rm com}$ is the energy (4) of corresponding commensurate phase at $T=0$. The critical temperatures of transitions are given by

$$kT_{\rm com}=-2E_{\rm com}. \tag{14}$$

After calculation of the maximal critical temperature from $T_{a,b}^{\pm}$ and $T_{\rm com}$, we obtain the resulting phase diagram as shown in Fig. 2 by solid lines. The symmetry of the diagram with respect to the change of sign of both interaction parameters κ and λ follows from the property (i) of the Hamiltonian (1).

To follow the evolution of this diagram when temperature decreases one should solve the infinite system of the coupled nonlinear variational equations obtained from the mean-field functional (5). The rigorous solution of this problem is beyond the scope of our study. However, qualitative aspects obtained in a more simple way are discussed below.

Note, first, that the stripe region of incommensurate phases in Fig. 2 appears at the same place where the infinite degenerate lines of phase transitions are predicted by the cluster calculations at $T=0$ (dotted lines). This indicates, similarly to the ANNNI model,[2,3] the devil's staircase behav-

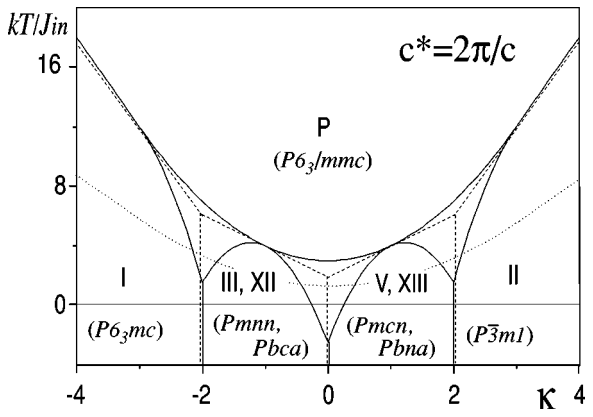

FIG. 4. Phase diagram of hcp-Ising model as function of the NN interaction parameter $\kappa = J_{\text{out}}/J_{\text{in}}$ and the reduced temperature kT/J_{in}, when the NNN interaction $J'_{\text{out}} = 0$. The transition from the paramagnetic (P) state to the commensurate phase (roman numbers) occurs either directly or via intermediate incommensurate phases $(q_a,0,0)$, $(q_a,0,c^*)$. Dashed lines correspond to the Kurzyński and Halawa [Phys. Rev. B **34**, 4846 (1986)] phase diagram. The σ^4 expansion of the free energy used for the construction of this diagram is applicable above the dotted line.

ior of the transition sequence below T_{inc}. An infinite number of lock-in phases, where the wave vector jumps between different rational multiples of the reciprocal-lattice periods, appear at low temperatures. Their phase boundaries converge to the dotted lines at $T=0$. Phases XII and XIII that are stable at low temperatures can appear from paramagnetic state only via intermediate incommensurate phases. The evolution of the incommensurate phases when temperature decreases is shown qualitatively in Fig. 4 for $J'_{\text{out}}=0$. The analogous phase diagram obtained in Ref. 13, when the possibility of an incommensurate phase was not considered, is shown in the same figure by the dashed lines.

The phase diagram of Fig. 4 is obtained within the approximation when the nonlinearity of the functional is modeled by the quartic terms of the Taylor expansion (6) and when the harmonic plane-wave approximation for the modulation is used. The incommensurate phase is described by a superposition of n harmonic plane waves with temperature-independent modulation wave vector, corresponding to the symmetry equivalent points in the q space and with equal real amplitudes σ_q. Either stripe phase with $n=1$ or double-modulated phases with $n=2$ or 3 are possible; in the $3q$ case, q_1, q_2, and q_3 form an equilateral 120° star. The harmonic approximation is as exact as T is closer to T_{inc}. Variation of q and contribution of higher harmonics at $T<T_{\text{inc}}$ is expected to be small and leads to a shift of the phase boundaries of the commensurate low-temperature phases towards the lower temperature as it happens in the ANNNI model.[1–3]

Under these approximations the energy of the incommensurate state (7) is written as

$$f_{\text{inc}} = nk(T-T_{\text{inc}})\sigma_q^2 + \frac{n}{2}kT\sigma_q^4 + n(n-1)kT\sigma_q^4, \quad (15)$$

or, after minimization over σ_q as

TABLE I. The lock-in wave vectors (q_a,q_b,q_c) and space symmetry groups of the commensurate phases appearing in the hcp-Ising model (see also Fig. 3). The correspondence between the notation of Ref. 10 used also in this paper and the notations used in Ref. 13 are given.

Notations (Ref. 10)	Notations (Ref. 13)	Lock-in vector (q_a,q_b,q_c)	Symmetry group
I	FP	(0,0,0)	$P6_3mc$
II	AP	$(0,0,2\pi/c)$	$P\bar{3}m1$
III	CP	$(0,2\pi/b,0)$	$Pmnn$
V	BP	$(0,2\pi/b,2\pi/c)$	$Pmcn$
XII		$(\pi/a,0,0)$	$Pbca$
XIII		$(\pi/a,0,2\pi/c)$	$Pbna$

$$f_{\text{inc}=} -\frac{1}{2}\frac{n}{2n-1}\frac{k}{T}(T-T_{\text{inc}})^2. \quad (16)$$

Note that Eq. (16) is minimal when $n=1$, i.e., $1q$ is the most stable incommensurate phase. Comparison of Eq. (16) at $n=1$ with the energy of corresponding commensurate phase obtained from Eq. (13), by minimization over σ

$$f_{\text{com}=} -\frac{3}{4}\frac{k}{T}(T-T_{\text{com}})^2, \quad (17)$$

gives the phase sequence below T_{inc}. When temperature decreases, the incommensurate phase is stable up to the temperature

$$T_c = T_{\text{inc}} - (3+\sqrt{6})(T_{\text{inc}}-T_{\text{com}}), \quad (18)$$

defined by the condition $f_{\text{inc}}=f_{\text{com}}$. Below T_c a first order transition occurs to one of the commensurate phases I, II, III, V, XII, or XIII. The region of $|\sigma| \ll 1$ where the above approximations are valid is placed above the dotted line on Fig. 4. Below this line one can get only qualitative ideas about the behavior of the transition boundaries.

IV. APPLICATION TO $A'A''BX_4$ COMPOUNDS

We use now the results of the hcp Ising model with competing interaction to study the high-temperature phase transitions in the $A'A''BX_4$ compounds provided by the vertical orientation of the apexes of the BX_4 tetrahedra. The calculated mean-field phase diagram (Fig. 2) reveals various incommensurate and lock-in phases that appear just below the transition and at lower temperatures. Some of the commensurate phases (I, II, III, and V) were discovered by Kurzyński and Halawa.[13] The occurring commensurate phases, their correspondence with notation of Ref. 13, their lock-in wave vectors, and corresponding symmetry groups are enumerated in Table I.

Our calculations reveal the following features of the phase diagram. The $1q$ basal-plane incommensurate phases directed either in the a or b crystallographic direction appear in the model. The direct first-order transition between phases I and V and between phases II and III is possible when NNN interaction is included. The new phases XII and XIII can occur at low temperatures.

TABLE II. The ratio c/a and the high-temperature sequences of transitions for several $A'A''BX_4$ compounds. A question mark signifies that either the information about the transitions at higher-temperature is not available or the melting occurs. The basal-plane incommensurate phase Inc has the modulation vector $(0,q_b,2\pi/c)$.

	c/a[a]	Transition sequence
K_2ZnCl_4	1.23	$\ldots - Pmcn - ?$
K_2WO_4	1.24	$\ldots - Pmcn - Inc - P6_3/mmc$
K_2CoCl_4	1.24	$\ldots - Pmcn - ?$
K_2CoBr_4	1.24	$\ldots - Pmcn - ?$
K_2MoO_4	1.24	$\ldots - Pmcn - Inc - P6_3/mmc$
Rb_2WO_4	1.25	$\ldots - Pmcn - Inc - P6_3/mmc$
K_2SeO_4	1.27	$\ldots - Pmcn - P6_3/mmc$
Rb_2MoO_4	1.27	$\ldots - Pmcn - ?$
$KNaSO_4$	1.29	$\ldots - P\overline{3}m1 - ?$
Cs_2WO_4	1.29	$\ldots - \overline{Pmcn} - ?$
Rb_2SeO_4	1.29	$\ldots - Pmcn - P6_3/mmc$
K_2SO_4	1.30	$\ldots - Pmcn - P6_3/mmc$
Cs_2MoO_4	1.30	$\ldots - Pmcn - ?$
K_2CrO_4	1.30	$\ldots - Pmcn - ?$
K_2MnO_4	1.30	$\ldots - Pmcn - ?$
$NaLiBeF_4$	1.34	$\ldots - Pmcn - ?$
Cs_2SO_4	1.37	$\ldots - Pmcn - P\overline{3}m1 - ?$
Rb_2SO_4	1.39	$\ldots - \overline{Pmcn - P\overline{3}m1} - ?$
$CsLiBeF_4$	1.62	$\ldots - Pmcn - ?$
$CsLiSO_4$	1.62	$\ldots - Pmcn - ?$
$RbLiSO_4$	1.64	$\ldots - Pmcn - ?$
$KLiBeF_4$	1.64	$\ldots - P6_3 - ?$
$KLiWO_4$	1.65	$\ldots - P6_3 - Cubic$
$KLiMoO_4$	1.67	$\ldots - P6_3 - Cubic$
$TlLiBeF_4$	1.68	$\ldots - P6_3 - ?$
$KLiSO_4$	1.69	$\ldots - P6_3 - Pmcn - P6_3/mmc$
$RbLiBeF_4$	1.69	$\ldots - P6_3 - ?$
$RbLiCrO_4$	1.70	$\ldots - P6_3 - Pmcn - P6_3/mmc$

[a]Since the ratio c/a for different compounds is given at different temperatures the error bars are estimated as ± 0.02 as the typical variation of thermal expansion. For compounds having an orthorhombic $Pmcn$ symmetry this ratio was estimated as $c/(ab/\sqrt{3})^{1/2}$.

Table II presents the high-temperature transition sequences for several typical $A'A''BX_4$ compounds and their correlation with the ratio c/a. (The data were collected on the basis of Refs. 4,14,25,26.) Only few compounds reveal the high-symmetry parent phase $P6_3/mmc$ associated with dynamically disordered BX_4 tetrahedra. One can imagine that in the other compounds the phase $P6_3/mmc$ is virtually present above the melting point.

According to their high-temperature transition sequence and to their ratio c/a the $A'A''BX_4$ compounds can be classified in a following way (see, also, Ref. 14):

(i) Located in the middle part of Table II are the non-underlined compounds with the direct transition (real or virtual) from the phase $P6_3/mmc$ to $Pmcn$ (phase V). Only a few compounds of this numerous group are given; for other examples see Refs. 4,14,25,26. Notably, for *all* the compounds of this group the ratio c/a varies from 1.27 to 1.64.

(ii) Located in the middle part of the Table II are the underlined compounds where the phase $P\overline{3}m1$ (phase II) occurs. Two of them, Cs_2SO_4 and Rb_2SO_4, demonstrate the reconstructive transition $Pmcn - P\overline{3}m1$. Compounds of this group have a similar ratio c/a as compounds of (i).

(iii) Located in the upper part of Table II are the alkali molybdates and tungstates K_2MoO_4, K_2WO_4, Rb_2WO_4 (Refs. 20–22) that have the intermediate incommensurate phase modulated along crystallographical direction b. The actual transition sequence there is: $Pmcn - (0,q_b,2\pi/c) - P6_3/mmc$. To our knowledge, there are no compounds with an a-directed incommensurate phase, although this phase already appears in the NN approximation. This group has the smallest ratios $c/a \simeq 1.23 - 1.25$. The other compounds of this group, K_2ZnCl_4, K_2CoCl_4, K_2CoBr_4, have a similar ratio c/a but the high-temperature phase $P6_3/mmc$ was not reported. They can be candidates for the basal-plane incommensurate phase if the melting does not precede the $Pmcn - Inc - P6_3/mmc$ transition.

(iv) Located in the lower part of Table II are compounds that demonstrate the phase $P6_3$ that is a subgroup of $P6_3mc$ (phase I). Several $A'A''BeF_4$ compounds and $KLiMoO_4$, with virtual $P6_3 - P6_3/mmc$ transition belong to this group. Two other compounds, $KLiSO_4$ and $RbLiCrO_4$, have the sequence $P6_3 - Pmcn - P6_3/mmc$.[27,14] These are particular systems since the complete vertical ordering of the tetrahedra occurs only in the room-temperature hexagonal phase $P6_3$. The orthorhombic phase $Pmcn$ is characterized by a partial vertical disorder of tetrahedra. These compounds reveal the reconstructive transition I-V. They can probably be considered as an intermediate case between classes (i) and (iii). Compounds of group (iv) have the largest ratios $c/a \simeq 1.64 - 1.70$.

Following Kurzyński and Halawa,[13] we assume that the sign and magnitude of J_{out} (and therefore of κ) depend critically on the ratio c/a. The interactions J_{in} and J'_{out} are less sensitive to variation of c/a. Compounds of groups (i), (iii), (iv) reproduce the phase diagram of Fig. 2 if one supposes that $\lambda < -0.5$ and that J_{out} changes its sign from negative (ferromagnetic) to positive (antiferromagnetic) when the hcp lattice goes from its expanded along the c axis form with $c/a > 1.63$, to the contracted form with $c/a < 1.63$. It is interesting to observe that the dipolar-dipolar interaction between two NN out-plane BX_4 tetrahedra changes its sign exactly at $c/a = 1.63$. The value of the modulation vector q_b in molybdates and tungstates is correlated with the ratio c/a in the following way: the smaller the ratio c/a the more q_b deviates from the lock-in value $2\pi/b$ of the phase $Pmcn$.[22] This behavior is consistent with our calculations (12). Compounds of the group (ii) seem to have a positive λ and are placed in the upper right corner of the diagram.

It would be interesting to study the evolution of the phase sequences in $A'A''BX_4$ compounds with a continuous variation of the interaction parameters. One can achieve this, e.g., by the application of uniaxial pressure along the hexagonal axes that slightly changes the ratio c/a. In particular, one can expect to obtain the commensurate-incommensurate transi-

tion, a-directed incommensurate phases, and the phase XII with symmetry $Pbca$ (or their subgroups). The classical compound K_2SeO_4 from group (i), having the smallest ratio $c/a=1.27$ could be a good candidate to achieve a Lifshitz point and a basal-plane incommensurate phase when submitted to an uniaxial pressure.

Another interesting result could be obtained by the application of an electrical field E along the hexagonal axis that breaks the mirror-basal-plane symmetry $S_i \rightarrow -S_i$ in the Hamiltonian (1). This results in the additional invariants $E\Sigma_i \sigma_i$ and $E\Sigma_i \sigma_i^3$ in the functional (6). The first one slightly favors the ferroelectric phase I. The second one gives the additional third-order term $E\Sigma \sigma_{q1}\sigma_{q2}\sigma_{q3}$ in Eq. (7) where the vectors q_1, q_2, q_3 form the equilateral triangle (calculations are analogous to those in Ref. 6). This would lead to the splitting of the transition $(0,q_b,2\pi/c)-P6_3/mmc$ into two transitions, with intervention of the $3q$ modulated incommensurate phase.

In our consideration an interaction with elastic degrees of freedom that is known to be important in ferroelectrics has been neglected. We expect that this coupling breaks the discontinuity of the transition from $P6_3/mmc$ to the low-temperature phase as it was observed in several $A'A''BX_4$ compounds. The corresponding analysis is currently in progress.

ACKNOWLEDGMENTS

We are grateful to N. Speziali for discussion of some experimental details. The work of I.L. was supported by the Brazilian Agency Fundacao de Amparo a Pesquisa em Minas Gerais (FAPEMIG) and by the Russian Foundation of Fundamental Investigations (RFFI), Grant No. 960218431a.

*Electronic address: lukyanc@itp.ac.ru.

†Present address: Department of Physics, Massachusetts Institute of Technology, Cambridge, Massachusetts 02139. E-mail: mpimenta@fisica.ufmg.br.

[1] T. Janssen, in *Incommensurate Phases in Dielectrics*, edited by R. Blinc and A. P. Levanyuk (North-Holland, Amsterdam, 1986), Vol. 1, p. 67.

[2] W. Selke, Phys. Rep. **170**, 213 (1988).

[3] W. Selke, in *Phase Transitions and Critical Phenomena*, edited by C. Domb and J. L. Lebowitz (Academic, New York, 1992), Vol. 15, p. 1.

[4] H. Z. Cummins, Phys. Rep. **185**, 211 (1990).

[5] P. Upton and J. Yeomans, Phys. Rev. B **40**, 479 (1989).

[6] K. Parlinski, S. Kwiecinski, and A. Urbanski, Phys. Rev. B **46**, 5110 (1992).

[7] K. Parlinski and G. Chapuis, Phys. Rev. B **47**, 13 983 (1993).

[8] K. Parlinski and G. Chapuis, Phys. Rev. B **49**, 11 643 (1994).

[9] M. A. Pimenta and P. Licinio, Phys. Rev. B **50**, 722 (1994).

[10] T. Kudo and Katsura, Prog. Theor. Phys. **56**, 435 (1976).

[11] R. McCormack, M. Asta, D. de Fontaine, G. Garbulsky, and G. Ceder, Phys. Rev. B **48**, 6767 (1993).

[12] J. Kanamori, J. Phys. Soc. Jpn. **53**, 250 (1984).

[13] M. Kurzyński and M. Halaway, Phys. Rev. B **34**, 4846 (1986).

[14] M. Kurzyński, Acta Phys. Pol. B **6**, 1101 (1995).

[15] B. Neubert and R. Siems, Ferroelectrics **185**, 95 (1996); M. Pleimling, B. Neubert, and R. Siems, Z. Phys. B **104**, 125 (1997).

[16] M. Kurzyński and M. Bratkowiak, J. Phys.: Condens. Matter **4**, 2609 (1992).

[17] Z. Y. Chen and M. B. Walker, Phys. Rev. Lett. **65**, 1223 (1990).

[18] Z. Y. Chen and M. B. Walker, Phys. Rev. B **43**, 5634 (1991).

[19] Y. Yamada and N. Hamaya, J. Phys. Soc. Jpn. **52**, 3446 (1983).

[20] A. J. van den Berg, F. Tuinstra, and J. Warczewski, Acta Crystallogr., Sect. B: Struct. Crystallogr. Cryst. Chem. **29**, 586 (1973).

[21] A. J. van den Berg, H. Overeijinder, and F. Tuinstra, Acta Crystallogr., Sect. B: Struct. Sci. **39**, 678 (1983).

[22] F. Tuinstra and A. J. van den Berg, Phase Transit. **3**, 275 (1983).

[23] C. Bichara, S. Crusius, and G. Inden, Physica B **182**, 42 (1992).

[24] P. Bak and J. von Boehm, Phys. Rev. B **21**, 5297 (1980).

[25] R. W. G. Wyckoff, *Crystal Structures* (Interscience, New York, 1965), Vol. 3.

[26] *Powder Diffraction File*, International Center for Diffraction Data, 1996, Pennsylvania 19073-3273.

[27] M. A. Pimenta, P. Echegut, Y. Luspin, G. Hauret, F. Gervais, and P. Abelard, Phys. Rev. B **39**, 3361 (1989).